

# 000 001 002 003 004 005 006 007 008 009 010 011 012 013 014 015 016 017 018 019 020 021 022 023 024 025 026 027 028 029 030 031 032 033 034 035 036 037 038 039 040 041 042 043 044 045 046 047 048 049 050 051 052 053 LLMPCA-DETECT: LLM-POWERED MULTIVARIATE FUNCTIONAL PCA FOR ANOMALY DETECTION IN SPARSE LONGITUDINAL TEXTS

Anonymous authors

Paper under double-blind review

## ABSTRACT

Sparse longitudinal (SL) textual data arises when individuals generate text repeatedly over time (e.g., customer reviews, occasional social media posts, electronic medical records across visits), but the frequency and timing of observations vary across individuals. These complex textual data sets have immense potential to inform future policy and targeted recommendations. However, because SL text data lack dedicated methods and are noisy, heterogeneous, and prone to anomalies, detecting and inferring key patterns is challenging. We introduce LLmFPCA-detect, a flexible framework that pairs LLM-based text embeddings with functional data analysis to detect clusters and infer anomalies in large SL text datasets. First, LLmFPCA-detect embeds each piece of text into an application-specific numeric space using LLM prompts. Sparse multivariate functional principal component analysis (mFPCA) conducted in the numeric space forms the workhorse to recover primary population characteristics, and produces subject-level scores which, together with baseline static covariates, facilitate data segmentation, unsupervised anomaly detection and inference, and enable other downstream tasks. In particular, we leverage LLMs to perform dynamic keyword profiling guided by the data segments and anomalies discovered by LLmFPCA-detect, and we show that cluster-specific functional PC scores from LLmFPCA-detect, used as features in existing pipelines, help boost prediction performance. We support the stability of LLmFPCA-detect with experiments and evaluate it on two different applications using public datasets, Amazon customer-review trajectories, and Wikipedia talk-page comment streams, demonstrating utility across domains and outperforming state-of-the-art baselines.

## 1 INTRODUCTION

In modern machine learning, it is common to encounter datasets comprising of  $N$  subjects, where each subject  $i$  is associated with a sequence of textual observations  $\{K_i(T_{i1}), K_i(T_{i2}), \dots, K_i(T_{iN_i})\}$  recorded at sparse and irregular time points  $\{T_{i1}, T_{i2}, \dots, T_{iN_i}\} \subset \mathbb{R}$ . Despite LLMs having spurred many advancements in analysis of text data, current methods are not well adapted to sparse longitudinal (SL) designs—time-evolving texts observed at irregular, subject-specific times—so these are frequently discarded or collapsed across time, ignoring the dynamic patterns in the texts. In this paper, we propose a novel framework for the analysis of SL text data that yields representations suitable for straightforward integration into unsupervised and supervised learning pipelines. The proposed methodology is applicable to a wide range of domains that generate SL text data, such as, electronic medical records in healthcare (Ford et al., 2016), consumer interactions through service channels in business (Cavique et al., 2022), activity logs from online learning platforms in education (Yang & Kang, 2020), user posts and comments on social media Hutto et al. (2013); Valdez et al. (2020); Kelley & Gillan (2022) and many more.

A major challenge with SL text datasets is that observations are unstructured and noisy, heterogeneous across subjects, and may contain outliers. The first step in making such data amenable for downstream supervised or unsupervised learning tasks, including prediction and inference, is to extract parsimonious feature representations of the longitudinal texts that capture the leading modes of variation. In this work, we propose LLmFPCA-detect, which starts from noisy SL texts and produces learned

054 representations, accounting for heterogeneity and providing type-I-error-controlled outlier screening.  
 055 LLmFPCA-detect begins by embedding text into an application specific numeric space using LLMs.  
 056 In this numeric space, sparse multivariate functional principal component analysis(mFPCA) Happ  
 057 & Greven (2018); Yao et al. (2005) is used to model the longitudinal text embeddings as noisy  
 058 observations of an underlying smooth trajectory. The method first clusters the preliminary FPC scores,  
 059 augmented with baseline subject-level covariates, and then screens for outliers; a novel calibration  
 060 step yields the final set of anomalies with statistical significance guarantees. We illustrate this new  
 061 approach on two datasets: the Amazon review corpus and the Wikipedia talk- page comment stream,  
 062 where LLmFPCA-detect reveals insightful findings from SL text data.  
 063

064 **Related Works** *Modeling SL data* Beginning with the seminal parametric random-effects formulation  
 065 Laird & Ware (1982), the field of longitudinal data analysis has undergone extensive development  
 066 over the decades; see Verbeke et al. (2014) for a review on multivariate longitudinal data analysis.  
 067 Functional data analysis (FDA) provides a nonparametric framework for SL data—via principal  
 068 components through conditional expectation Yao et al. (2005); Happ & Greven (2018)—to predict  
 069 subject-specific smooth trajectories even from one or a few observations. While this line of work has  
 070 expanded to include dynamic Hao et al. (2024); Zhou & Mueller (2024) and covariate-dependent Kim  
 071 et al. (2023) extensions, and has led to methods for clustering and unsupervised anomaly detection  
 072 Schmutz et al. (2020); Wu et al. (2023); Castrillón-Candás & Kon (2022), and supervised  
 073 tasks such as regression and classification Müller (2005), none of these methods extend directly to  
 074 heterogeneous, complex SL text data paired with baseline covariates and containing outliers.  
 075

076 *Text time series versus SL texts* An SL design differs from a time series; instead of a single, regularly  
 077 spaced sequence of observations, it comprises many subjects, each with its own trajectory recorded at  
 078 irregular, subject-specific times where per-subject sampling is sparse, and between-subject hetero-  
 079 geneity could be substantial. While text time-series modeling has advanced considerably O’Connor  
 080 et al. (2010); Blei & Lafferty (2006); Wang & McCallum (2006); Bamler & Mandt (2017); Dodds  
 081 et al. (2011); Griffiths & Steyvers (2004); Yurochkin et al. (2019), these approaches rely on dense,  
 082 uniformly spaced observations and are not suited to SL texts.  
 083

084 *Anomaly detection* Text clustering and anomaly detection are central NLP tasks, used to flag harmful  
 085 content, phishing, and spam. With pretrained language models (e.g., BERT Devlin et al. (2019),  
 086 RoBERTa Liu et al. (2019), GPT Brown et al. (2020)), embedding-based detectors have proliferated  
 087 alongside other approaches Yin & Wang (2016); Cao et al. (2025); Ruff et al. (2019); Subakti et al.  
 088 (2022); Dhillon & Modha (2001); Liu et al. (2008); Kannan et al. (2017). Yet three limitations  
 089 persist: (i) most methods lack type-I error control for flagged anomalies; (ii) time series anomaly  
 090 detectors Blázquez-García et al. (2021); Zamanzadeh Darban et al. (2024); Xu et al. (2022) can be  
 091 adapted to unstructured texts via embeddings, but only assuming dense, regularly sampled streams;  
 092 and (iii) these methods do not support SL designs with subject-specific, irregular observation times  
 093 and evolving trajectories, hence missing on the individual level dynamic trends in the anomalies.  
 094 Functional data analysis methods for SL anomaly detection exist (Sun & Genton, 2011; Dai & Genton,  
 095 2018; Hubert et al., 2015; Gervini, 2009), but they operate on structured numeric functions rather  
 096 than unstructured text and likewise lack formal false-positive guarantees. As a result, there is no  
 097 end-to-end solution that transforms SL texts into trajectory-aware feature representations and detects  
 098 anomalies with explicit type-I error control.  
 099

100 **Our Contributions** We introduce LLmFPCA-detect, a novel framework that combines LLM-based  
 101 embeddings with sparse mFPCA to enable covariate-informed data segmentation and type-I error  
 102 controlled anomaly detection in sparsely observed, longitudinal, heterogeneous text data, yielding  
 103 feature representations suitable for incorporating SL texts in a wide range of downstream tasks.  
 104 LLmFPCA-detect is broadly applicable to settings involving subjects with time-stamped text records  
 105 that arrive irregularly over time. While we focus on sparsely sampled scenarios, the methodology can  
 106 be readily adapted to densely observed data. We demonstrate the effectiveness of LLmFPCA-detect  
 107 through its application to the Amazon Reviews dataset (Amazon data) and the Wikipedia talk-page  
 108 comment streams (Wiki data). The key components of the framework, as illustrated in Figure 1, are:

1. **Representation** We derive domain-appropriate LLM embeddings for each time-stamped text. For  
 the Amazon Reviews dataset, we embed the texts using emotion scores based on Plutchik’s Wheel  
 of EmotionsPlutchik (1980), which identifies eight primary emotions as the foundation for all

108 others. For the Wikipedia request–comment stream, we obtain toxicity and aggression scores  
 109 using GPT for each comment to compare against findings from human-annotated scores.

110 2. **Learning trajectory representations and detection with guarantees** The numeric trajectories  
 111 form multivariate SL data, which are processed using the mFPCA pipeline to obtain multivariate  
 112 functional principal component (mFPC) scores. These scores, combined with baseline covariates,  
 113 are used for covariate-informed clustering. Anomalies are then detected in an unsupervised  
 114 manner by: i) screening points in the tails of the cluster-specific mFPC score distributions, and ii)  
 115 statistically testing the screened points while controlling for multiple comparisons. The identified  
 116 anomalies are further analyzed to localize time window specific deviations in the population.  
 117 3. **Interpretability and insights** We use LLMs to extract keywords from texts associated with each  
 118 cluster and flagged window, revealing dynamic, human-interpretable signals that explain why the  
 119 flagged discovery matters.

120 **Organization** The rest of the paper is organized as follows. Section 2 provides the motivation  
 121 for the clustering and anomaly detection steps of LLmFPCA-detect. Section 3 outlines the meth-  
 122 ods, estimation procedures, and algorithms that make up the different steps in LLmFPCA-detect.  
 123 Sections 4.1 and 4.2 demonstrates the application of LLmFPCA-detect to customer journey data  
 124 from Amazon reviews and to Wikipedia request–comment streams, illustrating its cross-domain  
 125 applicability. Additional details and experiments are provided in the Appendix.

## 127 2 MOTIVATION AND FRAMEWORK

129 In this section, we present the foundational framework underlying  
 130 LLmFPCA-detect.

132 **Multivariate functional data representation** For each subject  
 133  $i = 1, \dots, N$ , a random function  $\mathbf{X}_i \in L^2(\mathcal{T})^p$  is observed on  
 134 a discrete, potentially irregular and sparse time grid  $\{T_{ij}\}_{j,i=1}^{N_i, N}$   
 135 along with baseline covariates  $\mathbf{Z}_i \in \mathbb{R}^q$  where  $(\mathbf{X}, \mathbf{Z}) \sim \mathbb{P}$ ,  
 136 with  $\mathbb{P}$  being the joint distribution of  $(\mathbf{X}, \mathbf{Z})$ . The population  
 137 mean function is defined as  $\boldsymbol{\mu}(t) = \mathbb{E}(\mathbf{X}(t))$ , and the covariance  
 138 surface for  $s, t \in \mathcal{T}$  is given by  $\mathbb{C}(s, t) = \mathbb{E}\{(\mathbf{X}(s) - \boldsymbol{\mu}(s)) \otimes$   
 139  $(\mathbf{X}(t) - \boldsymbol{\mu}(t))\}$  with entries  $\mathbb{C}_{ij}(s, t) = \text{Cov}(X^{(i)}(s), X^{(j)}(t))$   
 140 is assumed to satisfy the conditions of Proposition 2 in Happ &  
 141 Greven (2018). Then,  $\mathbf{X}$  admits a multivariate Karhunen–Loève  
 142 expansion (Propositions 3 and 4 in Happ & Greven (2018))

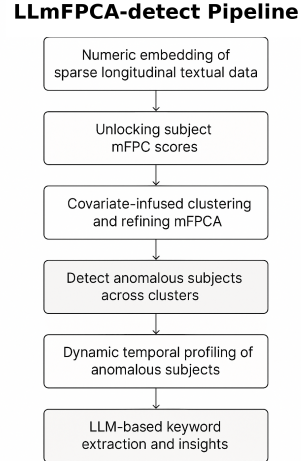
$$\mathbf{X}(t) = \boldsymbol{\mu}(t) + \sum_{j=1}^{\infty} \rho_j \boldsymbol{\psi}_j(t)$$

143 where  $\rho_j = \langle \mathbf{X}(t) - \boldsymbol{\mu}(t), \boldsymbol{\psi}_j(t) \rangle$  with  $\text{Cov}(\rho_j, \rho_n) = \lambda_j \mathbb{I}\{j = n\}$ , and  $\lambda_1 \geq \lambda_2 \geq \dots \geq 0$   
 144 are the eigenvalues of the covariance operator associated with  $\mathbb{C}$ . The corresponding eigenfunctions  
 145  $\boldsymbol{\psi}_j$ ,  $j \in \mathbb{N}$  serve as the multivariate functional principal components, with  $\rho_j$  being the associated  
 146 mFPC scores. If  $\mathbf{X}$  admits a finite expansion with  $M$  principal components, Proposition 5 in Happ &  
 147 Greven (2018) establishes how mFPCA of  $\mathbf{X}$  relates to univariate functional principal component  
 148 analysis (uFPCA) of each component  $X^{(d)}(\cdot) \in L^2(\mathcal{T})$  for  $d = 1, \dots, p$ .

149 **Data heterogeneity and anomalies** Suppose the trajectories  $\{\mathbf{X}_i\}_{i=1}^N$  belong to  $K$  distinct clusters,  
 150 denoted by  $\mathcal{C}_1, \dots, \mathcal{C}_K$ , with  $\bigcup_k \mathcal{C}_k = \{1, \dots, n\}$  and  $\mathcal{C}_k \cap \mathcal{C}_j = \emptyset$  for  $j \neq k$ . Observations in  $\mathcal{C}_k$   
 151 are generated according to the distribution  $\mathbb{P}_k$ , yielding the overall mixture  $\mathbb{P} = \sum_{k=1}^K \pi_k \mathbb{P}_k$  with  
 152  $(\pi_1, \dots, \pi_K)$  denoting cluster proportions. For  $i \in \mathcal{C}_k$ , assume that  $\mathbf{X}_i$  admits a finite multivariate  
 153 Karhunen–Loève expansion  $\mathbf{X}_i(t) = \boldsymbol{\mu}_k(t) + \sum_{m=1}^M \rho_{im} \boldsymbol{\psi}_m(t)$ ,  $i \in \mathcal{C}_k$ , where  $\boldsymbol{\mu}_k \in L^2(\mathcal{T})^p$  is  
 154 the cluster-specific mean function, and  $\boldsymbol{\psi}_m \in L^2(\mathcal{T})^p$  are shared eigenfunctions across clusters. To  
 155 incorporate possible measurement errors and anomalies, we observe

$$\mathbf{Y}_i(t) = \mathbf{X}_i(t) + \boldsymbol{\eta}_i(t) + \mathbf{a}_i(t),$$

156 where  $\boldsymbol{\eta}_i, \mathbf{a}_i \in L^2(\mathcal{T})^p$  capture the measurement errors and anomalies respectively. These are  
 157 assumed to be jointly independent of  $\mathbf{X}_i$ ,  $i = 1, \dots, n$ , with  $\mathbb{E}(\boldsymbol{\eta}_i(t)) \equiv 0$  for all  $t \in \mathcal{T}$ , and



159 Figure 1: Proposed framework

162  $\text{Cov}(\eta^{(j)}(s), \eta^{(k)}(t)) = \sigma_\eta^2 \mathbb{I}_{s=t}$  for all  $j, k \in \{1, \dots, p\}$ . The term  $\mathbf{a}_i \equiv \mathbf{0}$  almost surely for all  
 163  $i \in \mathcal{A}_0^C$ , where  $\mathcal{A}_0 \subset \{1, \dots, N\}$  denotes the set of anomalous subjects. For each  $i \in \mathcal{A}_0$ , we  
 164 assume  $\mathbf{a}_i(t) \neq \mathbf{0}$  for some  $t \in \mathcal{T}_0 \subset \mathcal{T}$  almost surely. We employ trimmed  $k$ -means to recover  
 165 the clusters accurately despite being contaminated with outliers; for details on cluster recovery see  
 166 Section D.1 in Appendix D.

167 **Calibrating the anomalies** After the clusters are recovered, the anomalous observations in  $\mathcal{A}_0$  are  
 168 assigned to one of the clusters  $\mathcal{C}_1, \dots, \mathcal{C}_K$ . To detect  $\mathcal{A}_0$  in an unsupervised manner, we perform a  
 169 screening step within each cluster by examining the tails of the FPC score distribution, approximating  
 170  $\mathcal{C}_k \cap \mathcal{A}_0$  by  $\mathcal{A}_0^{k,\epsilon} \subset \mathcal{C}_k$  (see Appendix E). The distribution of FPC scores in the clean subset  $\mathcal{C}_k \cap \mathcal{A}_0^C$   
 171 is then used to recover  $\mathcal{C}_k \cap \mathcal{A}_0$  with confidence. In practice, each cluster  $\mathcal{C}_k$  is randomly split into  
 172 two subsets, and the non-screened portion is used to calibrate the anomaly detection procedure; see  
 173 Theorem E.1 in Appendix E for theoretical guarantees. Finally, based on the detected anomalous set  
 174  $\mathcal{A}_0$ , we analyze the corresponding keywords across different time windows.

175 The foregoing framework outlines a pipeline for obtaining cluster-specific feature representations  
 176 and type-I controlled anomaly detection in fully observed multivariate functional trajectories with  
 177 possible measurement errors. In SL settings, each subject is observed at random time points  $T_{ij}$  for  
 178  $i = 1, \dots, N, j = 1, \dots, N_i$ , with  $T_{ij} \in \mathcal{T}$ . These time points  $T_{i1}, \dots, T_{iN_i}$  are assumed i.i.d. and  
 179 independent of  $\mathbf{X}_i$  and  $\boldsymbol{\eta}_i$  for all  $i$ . The number of measurements  $N_i$  is random, reflecting sparse  
 180 and irregular designs, and  $N_i$ , for  $i = 1, \dots, N$ , are assumed i.i.d. and independent of all other  
 181 random elements. In practice, we observe  $Y_i(T_{ij})$ ,  $j = 1, \dots, N_i$ ,  $i = 1, \dots, N$ , and all relevant  
 182 quantities must be estimated from these noisy observations. Section 3 outlines the estimation details  
 183 and algorithms for this pipeline, including steps for incorporating the underlying textual data.

### 185 3 METHODS: PIPELINE AND ESTIMATION

187 **From SL Texts to Numeric Embeddings** The first step maps each time-stamped text  $K_i(T_{ij})$  to a  
 188  $p$ -dimensional vector via a fixed embedding

$$189 \Phi : \mathcal{X} \longrightarrow \mathbb{R}^p, \quad \mathbf{Y}_i(T_{ij}) = \Phi(K_i(T_{ij})), \quad (1)$$

190 where  $\Phi$  is implemented via LLM prompting, held constant across subjects, and deterministic (the  
 191 same text yields the same vector). For subject  $i$  this yields the multivariate trajectory  $\{\mathbf{Y}_i(T_{ij})\}_{j=1}^{N_i}$ ,  
 192 whose coordinates are modeled jointly using mFPCA (e.g. Plutchik emotion embeddings for Amazon  
 193 reviews; see Sections C and 4.1). Each subject also has baseline, time-invariant covariates  $\mathbf{Z}_i \in \mathbb{R}^q$   
 194 (e.g. average rating, review length, engagement duration).

---

#### 196 197 **Algorithm 1** Multivariate Functional Principal Component Analysis (mFPCA)

---

198 **Input:** SL data:  $\{\mathbf{Y}_i(T_{ij})\}_{j=1}^{N_i}$  for  $i = 1, \dots, N$ .

- 199 1:  $(\{\xi_{ik}^{(d)}\}_{i=1, k=1}^{N, K_d}, \hat{\mu}^{(d)}(t), \{\hat{\phi}_k^{(d)}(t)\}_{k=1}^{K_d}) \leftarrow \text{uFPCA}(\{(T_{ij}, Y_i^{(d)}(T_{ij}))\}_{i,j})$  for each dimension  
 200  $d = 1, \dots, p$ . ▷ Algorithm 4; only scores are used below
- 201 2:  $\hat{\mathbf{\Xi}}_i \leftarrow (\hat{\xi}_{i1}^{(1)}, \dots, \hat{\xi}_{iK_1}^{(1)}, \dots, \hat{\xi}_{i1}^{(p)}, \dots, \hat{\xi}_{iK_p}^{(p)}), i = 1, \dots, N$  ▷ Stack univariate FPC scores
- 202 3: Define matrix  $\hat{\mathbf{\Xi}} \in \mathbb{R}^{N \times M}$  with rows  $\hat{\mathbf{\Xi}}_i$  where  $M = \sum_{d=1}^p K_d$ .
- 203 4:  $\hat{\mathbf{C}}_{\Xi} \leftarrow \frac{1}{N-1} \hat{\mathbf{\Xi}}^T \hat{\mathbf{\Xi}}$ . ▷ Compute covariance matrix
- 204 5: Perform eigen-decomposition of  $\hat{\mathbf{C}}_{\Xi}$  to obtain eigenvalues  $\{\hat{\lambda}_m\}_{m=1}^M$  and eigenvectors  
 205  $\{\hat{\mathbf{v}}_m\}_{m=1}^M$ .
- 206 6:  $\hat{\psi}_m^{(d)}(t) \leftarrow \sum_{k=1}^{K_d} \hat{v}_{m,k}^{(d)} \hat{\phi}_k^{(d)}(t)$ ,  $d = 1, \dots, p$  and  $m = 1, \dots, M$ . ▷ Multivariate eigenfunctions
- 207 7:  $\hat{\rho}_{im} \leftarrow \hat{\mathbf{\Xi}}_i^T \hat{\mathbf{v}}_m$  for  $i = 1, \dots, N$  and  $m = 1, \dots, M$  ▷ Compute mFPC scores

210 **Output:** Tuple of estimated mFPC scores, eigenfunctions and mean curves:  $\{\hat{\rho}_{im}, \hat{\psi}_m, \hat{\mu}\}_{i,m=1}^{N,M}$ .

---

212 **Dynamic Trajectory Representations using mFPCA** Algorithm 1 details the estimation steps  
 213 of the mFPCA setup outlined in Section 2. Starting from  $\{\mathbf{Y}_i(T_{ij})\}_{j=1}^{N_i}$ , we estimate the mFPC  
 214 scores  $\hat{\rho}_{im}$  by building on the univariate functional principal component analysis (uFPCA) of each  
 215  $\{Y_i^{(d)}(T_{ij})\}_{j,i=1}^{N_i, N}$  for  $d = 1, \dots, p$ . The algorithm follows the approach in Happ & Greven (2018),

216 using estimated quantities from uFPCA including the mean functions  $\hat{\mu}^{(d)}(t)$ , eigenfunctions  $\hat{\phi}^{(d)}(t)$   
 217 and univariate FPC scores  $\hat{\xi}_{ik}^{(d)}$ ; for details see Algorithm 4 in Section C.2 and Yao et al. (2005).  
 218

---

**220 Algorithm 2** Detecting anomalous subjects within a cluster  $\hat{\mathcal{C}}$ 

221 **Input:** Subject cluster  $\hat{\mathcal{C}}$ ; data  $\{\mathbf{Y}_i(T_{ij}) : i \in \hat{\mathcal{C}}\}$ ; significance levels  $\alpha_1, \alpha$  (where  $\alpha_1 > \alpha$ ).  
 222

- 223 1: Obtain mFPC scores  $\{\hat{\rho}_{im}^{\hat{\mathcal{C}}}\}_{i \in \hat{\mathcal{C}}, m=1, \dots, B}$  corresponding to the top  $B$  cluster-specific mFPC  
 224 components using Algorithm 6 applied to  $\{\mathbf{Y}_i(T_{ij}) : i \in \hat{\mathcal{C}}\}$ .  
 225  $\triangleright B$ : number of top mFPC components based on prop. of variance explained
- 226 2: Randomly partition  $\hat{\mathcal{C}}$  into disjoint sets  $I_1, I_2$  of equal size.
- 227 3:  $(G_1, G_1^c) \leftarrow \text{ScreenPotentialOutliers}(I_1, \{\hat{\rho}_{im}^{\hat{\mathcal{C}}} : j \in I_1\}, B, \alpha_1)$ .  $\triangleright$  Algorithm 7
- 228 4:  $(G_2, G_2^c) \leftarrow \text{ScreenPotentialOutliers}(I_2, \{\hat{\rho}_{im}^{\hat{\mathcal{C}}} : j \in I_2\}, B, \alpha_1)$ .
- 229 5: Initialize  $\mathcal{A}^{(1)} \leftarrow \emptyset$ .  $\triangleright$  Set of confirmed outliers for cluster  $\hat{\mathcal{C}}$
- 230 6:  $\mathcal{A}_{G_1}^{(1)} \leftarrow \text{ConfirmAnomalies}(G_1, G_2^c, \{\hat{\rho}_{im}^{\hat{\mathcal{C}}} : j \in G_1 \cup G_2^c\}, B, \alpha)$ .  $\triangleright$  Algorithm 8
- 231 7:  $\mathcal{A}_{G_2}^{(1)} \leftarrow \text{ConfirmAnomalies}(G_2, G_1^c, \{\hat{\rho}_{im}^{\hat{\mathcal{C}}} : j \in G_2 \cup G_1^c\}, B, \alpha)$ .
- 232 8:  $\mathcal{A}^{(1)} \leftarrow \mathcal{A}_{G_1}^{(1)} \cup \mathcal{A}_{G_2}^{(1)}$ .

233 **Output:** Set of confirmed anomalous subjects  $\mathcal{A}^{(1)} = \{(i, S_i) : i \in \hat{\mathcal{C}} \text{ is an outlier}, S_i \neq \emptyset\}$ .  
 234

---

235  
 236  
 237 **Clustering and Anomaly Detection using mFPC Scores and Covariates** We segment subjects by  
 238 clustering their estimated mFPC scores jointly with static covariates (Algorithm 5, Appendix D). For  
 239 each estimated cluster  $\hat{\mathcal{C}}_k$  we re-fit mFPCA using only its members (Algorithm 1; Algorithm 6), yielding  
 240 cluster-specific means  $\hat{\mu}_k(t)$ , eigenfunctions  $\hat{\psi}_m^k(t)$ , updated scores  $\hat{\rho}_{im}^k$  and reconstructed  
 241 trajectories (Equation equation 8).  
 242

---

**243 Algorithm 3** Dynamic temporal profiling of anomalous subjects

244 **Input:** Type 1 anomalies  $\mathcal{A}^{(1)}$  (from Alg. 2 for cluster  $\hat{\mathcal{C}}$ ); data  $\{\mathbf{Y}_j(T_{jk}) : j \in \hat{\mathcal{C}}\}$ ; cluster means  
 245  $\{\hat{\mu}_{\hat{\mathcal{C}}}^{(d)}(t)\}$  (from Alg. 6); Clean held-out sets  $G_1^c, G_2^c$  & split info  $I_1, I_2$  for  $\hat{\mathcal{C}}$  (from Alg. 2); time  
 246 windows  $\{(a_w, b_w)\}_{w=1}^W$ ; significance level  $\alpha$ .  
 247

- 248 1:  $(\{\bar{\mu}_{\hat{\mathcal{C}}}^{(w)}\}_{w=1}^W, \{D_j^{(w)}\}_{j \in G_1^c \cup G_2^c, w=1, \dots, W}) \leftarrow \text{ComputeWindowDeviations}(\{\mathbf{Y}_j(T_{jk}) : j \in G_1^c \cup G_2^c, \{ \hat{\mu}_{\hat{\mathcal{C}}}^{(d)}(t)\}, \{(a_w, b_w)\}_{w=1}^W)$ .  $\triangleright$  Compute scores for clean held-out set Alg. 9
- 249 2:  $\mathcal{A}^{(2)} \leftarrow \text{IdentifyAnomalousWindows}(\mathcal{A}^{(1)}, \{\mathbf{Y}_i(T_{ij}) : i \text{ s.t. } (i, \_) \in \mathcal{A}^{(1)}\},$
- 250  $\{\bar{\mu}_{\hat{\mathcal{C}}}^{(w)}\}, \{D_j^{(w)}\}, I_1, I_2, G_1^c, G_2^c,$   
 251  $\{(a_w, b_w)\}_{w=1}^W, \alpha)$ .  $\triangleright$  Identify anomalous windows for subjects (Alg. 10)

252 **Output:** Set of subject-indexed anomalous temporal windows  $\mathcal{A}^{(2)} = \{(i, \mathcal{W}_i) : i \in \mathcal{A}^{(1)}, \mathcal{W}_i \neq \emptyset\}$ .  
 253

---

254 Globally anomalous subjects will still be assigned to one of the  $K$  clusters unless explicitly  
 255 screened—a difficult task in heterogeneous data. To detect such cases post-assignment, we apply  
 256 Algorithm 2 (with Algorithms 7 and 8; Appendix E). The procedure tests whether a subject’s  
 257 multivariate FPC scores deviate from the typical pattern of its assigned cluster  $\hat{\mathcal{C}}$ , using sample  
 258 splitting and data-driven calibration to control multiplicity across principal components. It outputs  
 259 flagged subjects  $\mathcal{A}^{(1)} = (i, S_i)$ , where  $S_i$  records the outlying FPC directions—information that then  
 260 guides localized anomaly analysis (Algorithm 3).  
 261

262 Subjects flagged by Algorithm 2 (set  $\mathcal{A}^{(1)}$ ) may be anomalous only over portions of their trajectories.  
 263 Algorithm 3 localizes these periods by comparing each subject’s raw segments to the cluster mean,  
 264 with data-driven calibration (Algorithm 9); implementation details are in Appendix E (Algorithms 9,  
 265 10). The output is  $\mathcal{A}^{(2)} = (i, \mathcal{W}_i)$ , where  $\mathcal{W}_i$  denotes the time windows in which subject  $i$ ’s trajectory  
 266 departs from a clean cohort within that window. This step pinpoints atypical intervals and enables  
 267 per-window anomaly flags, which feed into the final dynamic keyword profiling stage.  
 268

270 **Dynamic Keyword Profiling** Finally, we describe intent extraction from anomalous reviews. For  
 271 each subject  $i$ , let  $S_i$ , be the anomalous reviews. Challenges include lexical variation for similar  
 272 semantics, shared stylistic drift across users, and scalability for large number of anomalous reviews.  
 273 We maintain a time-ordered intent list  $I_i^{(t-)}$  from reviews before time  $t$ . At time  $t$ , an LLM receives  
 274  $I_i^{(t-)}$ , top global intents observed before  $t$ , and the current review, and either matches an existing  
 275 intent or proposes a new one. Full details appear in Algorithm 11 (Appendix F).  
 276

## 277 4 REAL DATA APPLICATIONS

### 279 4.1 MODELING DYNAMIC EMOTIONS IN AMAZON CUSTOMER REVIEWS

281 We use the Amazon Reviews corpus Hou et al. (2024), which in-  
 282 cludes 1,946 users and 22,032 reviews over five years, focusing  
 283 on Automobile for the main analysis; Beauty & Personal Care and  
 284 Sports & Outdoors supply user-level covariates (e.g., cross-category  
 285 purchase share). Each review includes a user ID, timestamp, product  
 286 title, text, and a 1–5 rating, with users posting over multiple years.  
 287

288 **Emotion embedding for text transcripts** Plutchik’s wheel of  
 289 emotions provides a structured framework for mapping emotional  
 290 states along opposing pairs, capturing both intensity and polarity  
 291 (see Fig. 2 Semeraro et al. (2021)). We convert each transcript into  
 292 four real-valued scores—joy–sadness, trust–disgust, fear–anger, and  
 293 surprise–anticipation—on a continuous  $[-1, 1]$  scale, where  $-1$  and  
 294  $1$  denote the extremes of each pole (e.g., grief vs. ecstasy), and  
 295 intermediate values encode moderate intensity. A zero-shot GPT-3.5-  
 296 Turbo prompt returns one scalar per axis (details and validation in Section C.1). Stacking these over  
 297 time yields a 4-D timestamped embedding per subject, which serves as the input to LLmFPCA-detect  
 for mFPCA and the subsequent steps.  
 298

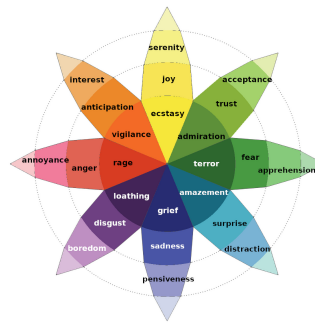
299 Rating	300 Review	301 Joy–Sadness	302 Trust–Disgust	303 Fear–Anger	304 Surprise–Anticipation
300 5	301 I use this great oil in all of my 150cc Scooters (was told to by a Scooter 302 mechanic) and I've never had an engine problem. But this price is thru the 303 roof, \$17.50 for a single quart is STUPID...wally world sells it for \$4.99...but 304 its kinda funny that all of Amazon's oils are priced thru the roof	-0.8	-0.6	-0.8	-1
300 1	301 Received this today and went to put it on my 3/8 extension for an oil filter 302 change. The machining is pretty, but measurements are so poor I cannot get 303 it on the extension to use. Absolute junk! I should have paid more attention 304 to the negative review.	-0.77	-0.75	-0.5	-0.7

305 Table 1: Amazon customer reviews with emotion scores across four Plutchik dimensions.  
 306

307 Table 1 illustrates how emotion embeddings reveal customer pain points that are not captured by  
 308 5-star ratings alone. In the first example, a 5-star review shows strong sadness ( $-0.8$ ), disgust ( $-0.6$ ),  
 309 anger ( $-0.8$ ), and surprise ( $-1$ ), indicating frustration with pricing despite overall satisfaction. The  
 310 third example, also rated 1 star, shows high sadness ( $-0.77$ ), disgust ( $-0.75$ ), and surprise ( $-0.7$ ),  
 311 pointing to severe frustration over usability issues.  
 312

313 **Emotion mFPCA scores (Algorithm 1) improve predictive power over product ratings** We test  
 314 whether review text improves forecasting of adverse outcomes (e.g., sudden rating drops) in Amazon  
 315 Reviews. A “rating drop” is defined as the extreme percentile of each user’s maximum gap between  
 316 consecutive ratings. We compare two optimally tuned random-forest models on a class-balanced  
 317 sample with identical baseline covariates—cluster labels from Algorithms 1–5 and purchase mix  
 318 across categories. Model A summarizes past behavior by the mean Automobile rating; Model B  
 319 replaces that single aggregate with emotion mFPC scores, capturing time-varying textual signals.  
 320 On the test set, Model A: accuracy 0.542, precision 0.538, recall 0.596, F1 0.565, ROC–AUC 0.534.  
 321 Model B improves all metrics—accuracy 0.609 (**+12.4%**), precision 0.610 (**+13.4%**), recall 0.603  
 322 (**+1.2%**), F1 0.606 (**+7.3%**), ROC–AUC 0.645 (**+20.8%**)—showing that compact emotion-trajectory  
 323 features capture predictive signal beyond coarse star-rating averages.

324 **Clustering dynamics and case studies** Figure 3 plots mean emotion trajectories for the three clusters  
 325 from purchasing proportions in Automobiles, Beauty & Personal Care, and Sports & Outdoors).



326 Figure 2: Plutchik’s wheel of  
 327 emotions

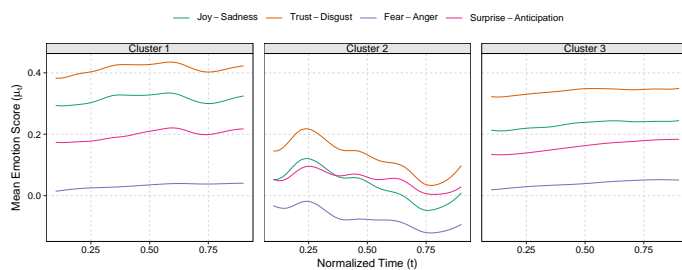


Figure 3: Mean emotion trajectories across the three user clusters. Curves represent mean scores for the Joy–Sadness, Trust–Disgust, Fear–Anger, and Surprise–Anticipation emotion dimensions.

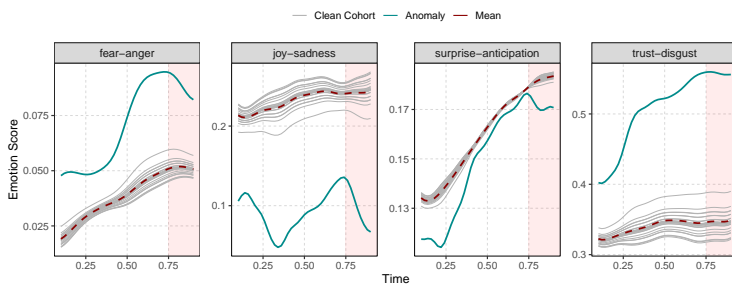


Figure 4: Mode of variation plot for a user along the fourth FPC (outlying) from cluster 3

Cluster 1 has the highest baseline across emotions—consistently stronger affect. Cluster 3 follows a similar temporal shape but is uniformly lower (milder affect). Cluster 2 departs most, with elevated sadness and anger, indicating sharper pain points. Because anomalies are scored relative to each cluster’s mean, even upward shifts in positive emotion within Cluster 2 can register as anomalous. Section D.3 of the Appendix reports bootstrap analysis confirming cluster stability.

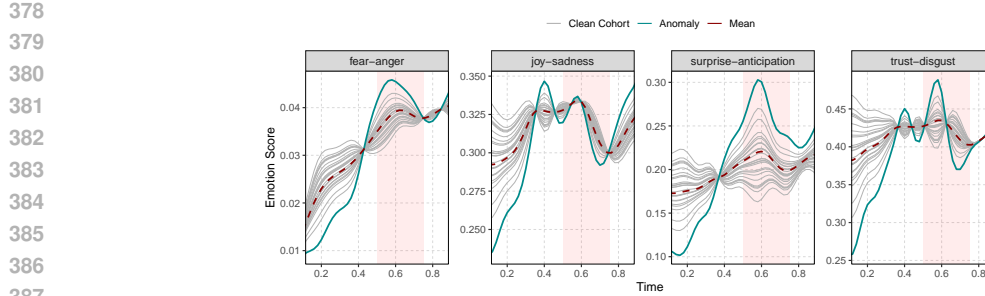
Through mode-of-variation plots (see Section C.2 for details) and corresponding review excerpts in the flagged time window, we show that the detected anomalies capture customer pain points. Figure 4 shows a user’s emotional trajectory relative to Cluster 3. The user’s emotions are consistently shifted from the cluster mean along the fourth eigenfunction in Cluster 3, with a pronounced spike in the fear-anger petal and a sharp drop in joy–sadness during the final time window—signaling a clear pain point. Review texts from this period reveal issues with mismatched parts, specifically a replacement door-handle cover with incorrect keyhole cut-outs. The dominant complaints relate to product fit and quality control. These insights suggest actionable interventions, such as enforcing compatibility checks at purchase and improving final-stage quality control by the seller.

Figure 5 shows a user exhibiting a dip–recovery emotional pattern along the second eigenfunction. Early in the timeline, all four emotion petals remain well below the cluster baseline. During the anomalous time window, there is a sharp rise in fear and surprise, driven by issues related to poor product quality. The user expresses frustration and regret, suggesting loss of brand trust. Key pain points include the failure of a critical component and confusion caused by missing documentation.

**Keyword profiling** After detecting anomalies, we perform keyword profiling (Algorithm 11 in Section F of the Appendix) to each flagged instance. Table 2 summarizes the keywords associated with anomalous points in each cluster. A quick glance shows that users in Cluster 2 tend to express broadly negative emotions, while Cluster 3 highlights more specific issues—such as missing cables and poor documentation—reflecting the more descriptive and varied nature of reviews in that group. Table 6 illustrates dynamic profiling of keywords; see Section F in the Appendix for details.

## 4.2 TRACKING TOXICITY AND AGGRESSION IN WIKIPEDIA REQUEST–COMMENT STREAM

We evaluate LLmFPCA-detect on the English Wikipedia request–comment stream to demonstrate cross-domain applicability. For each comment, we record the text, timestamp, structured user

388 Figure 5: Mode of variation plot for a user along the second FPC (outlying) from cluster 1  
389

390

Cluster	Keywords
Cluster 1	as described, good quality, perfect product, poor value for money, wrong size, poor fit
Cluster 2	poor quality, poor value for money
Cluster 3	as described, bulky design, good quality, good value for money, good design, leaks fuel, missing cable, quantity issue, poor documentation, wrong size

397 Table 2: Group-level pain points detected across clusters  
398  
399

400 covariates, and crowdsourced ground-truth toxicity/aggression scores. This corpus exemplifies sparse  
401 longitudinal text: users post at irregular, infrequent intervals. The dataset was collected via the  
402 Wikipedia API, restricted to the user-talk and article-talk namespaces, and sourced from Wiki data.  
403 We retain comments from 2010–2015 authored by 925 pseudonymized users.

404

Method	TW1	TW2	TW3	TW4	TW5
LLmFPCA-detect (gpt-4o-mini)	<b>0.58</b>	<b>0.58</b>	<b>0.46</b>	<b>0.37</b>	<b>0.32</b>
Isolation Forest (BERT)	0.41	0.33	0.25	0.23	0.39
Isolation Forest (gpt-4o-mini)	0.41	0.33	0.25	0.23	0.39

410 Table 3: F1 scores for anomalies detected by LLmFPCA-DETECT versus ground truth, compared  
411 with Isolation Forest on GPT-derived scores and a BERT baseline (segregated by time windows).  
412

413 **Comparison with state-of-the-art** We assess anomaly detection on Wikipedia by treating human-  
414 annotated toxicity/aggression as surrogate ground truth and extracting GPT-derived toxicity/ag-  
415 gression scores from text via prompts. As a content-agnostic baseline, we use BERT embeddings  
416 (no explicit toxicity cues). We partition the timeline into five windows and, within each, define  
417 pseudo-ground-truth anomalies using Isolation Forest on the human scores plus user covariates  
418 (comment count, median inter-comment gap). We then run Isolation Forest on (i) GPT-derived  
419 scores and (ii) BERT embeddings (each with the same covariates) as baselines. Finally, we apply  
420 LLmFPCA-detect to the GPT-derived trajectories with the same covariates to flag anomalies across  
421 the five windows and compare against these baselines (Table 3).

422 **Cluster dynamics** LLmFPCA-detect flags not only one-off vandalism or brief flare-ups by otherwise  
423 well-behaved contributors, but also sustained problematic behavior and its mode of deviation. For  
424 example, Cluster 1 outliers tend to post unusually high volumes or engage in extended policy disputes,  
425 whereas Cluster 2 outliers show short, intense bursts of toxic language. Table 4 presents representative  
426 cases with brief excerpts and the corresponding anomalous time window. In Cluster 1, the dominant  
427 pattern is procedural friction—disagreements about process (e.g., whether a proposed mentorship  
428 program requires further consensus) rather than direct attacks. By contrast, Cluster 2 features  
429 overt hostility, where procedural disagreements escalate into personal or confrontational language.  
430 Additionally, Appendix D.3 reports bootstrap analyses confirming stability of the obtained clusters.

431 **Keyword profiling** Dynamic keyword profiling makes each anomaly interpretable (Table 5). Rather  
than an opaque outlier score, moderators see the top terms that triggered the flag, revealing the

432	Cluster	User ID	Comment excerpt (abridged)	Label
433	1	10783082	“...If that’s how you want it. I will talk to this to ANI if necessary ...”	1
434	1	10756369	“== Adopt Me == Here is a proposal for a new mentorship process ...”	1
435	2	2305952	“OK, maybe I was wrong. I’m sorry, but don’t try me again ...”	5
436	2	2305952	“No, that’s irrelevant. Your source is garbage, stop spamming it.”	5
437				
438				

439 Table 4: Examples from the Wikipedia comment stream where detected anomalies match crowd-  
 440 sourced annotations, showing cluster ID, anonymized user ID, excerpt, and toxicity/aggression label.  
 441

442	Cluster 1 (Window)	Top keywords (LLmFPCA-detect)	Theme
443	W1	consensus, policy, “WP: ANI”	Policy enforcement friction
444	W2	civility, manners, please, courtesy	Soft-skills reminders
445	W3	backlog, deadline, stall, formalise	Procedural urgency
446	Cluster 2 (Window)	Top keywords (LLmFPCA-detect)	Theme
447	W4	nonsense, garbage-source, stop-spamming	Direct hostility
448	W5	revert, vandal, warning, block, “3RR”	Conflict over content
449	W5	wasting-time, already-explained	Moderator fatigue
450			
451			
452			
453			

454 Table 5: Dynamic–keyword profiling makes each anomaly legible. In this Wikipedia setting, instead  
 455 of an opaque outlier score, the moderator sees the top keywords that drove the statistical flag.  
 456

457  
 458 concerns underlying anomalous behavior. In this corpus, Cluster 1 anomalies are predominantly  
 459 procedural—e.g., disputes over which venue (WP:ANI, etc.) should adjudicate. Cluster 2, by contrast,  
 460 exhibits explicit antagonism: personal attacks, contempt for sources (“garbage-source”), and edit-war  
 461 jargon. The exasperation lexicon (“wasting time,” “already explained”) further signals moderator  
 462 fatigue—an operational risk that steady-state toxicity metrics would miss.  
 463

464 Identifying peak–hostility windows (e.g., Window 5) with LLmFPCA-detect enables proactive  
 465 moderation, such as temporarily throttling edits. In Cluster 1, the dominant issue is procedural  
 466 friction, suggesting policy fixes like clearer closure rules or targeted sanctions. Keyword profiling  
 467 pinpoints specific, time-bounded situations where light-touch actions can prevent rule violations  
 468 and burnout. Linking time windows to salient terms reveals root causes and supports proportionate,  
 469 domain-specific responses instead of one-size-fits-all bans.  
 470

## 471 5 CONCLUSION

472  
 473 LLmFPCA-detect provides an end-to-end framework for sparse longitudinal (SL) text by integrating  
 474 LLM-embeddings with functional data analysis. LLmFPCA-detect tackles key challenges in such  
 475 datasets—including sparsity, irregularity, noise, and semantic complexity—by embedding text into  
 476 meaningful numeric representations, followed by mFPCA which is used for user segmentation,  
 477 anomaly detection, and dynamic intent profiling across large SL text datasets, a setting that remains  
 478 largely unaddressed in the literature. Applied to Amazon customer reviews, LLmFPCA-detect  
 479 successfully uncovers emotion dynamics and identifies critical pain points in the customer journey,  
 480 offering valuable insights for consumer analytics. We demonstrate the utility of LLmFPCA-detect on  
 481 English Wikipedia request–comment stream to detect toxic comments, where the detected anomalies  
 482 align well with crowdsourced human annotations. The flexibility of LLmFPCA-detect makes it  
 483 applicable to other domains such as healthcare, education, and social media where SL text data  
 484 is routine. Future work includes establishing theoretical guarantees based on mFPCA estimates  
 485 rather than fully observed trajectories, and extending LLmFPCA-detect to other supervised and  
 unsupervised tasks on SL text datasets.

486 REFERENCES  
487

488 Hussam Alhuzali and Sophia Ananiadou. Spanemo: Casting multi-label emotion classification as  
489 span-prediction. In *Proceedings of the 2021 Conference of the North American Chapter of the*  
490 *Association for Computational Linguistics: Human Language Technologies*, pp. 1571–1585, 2021.

491 Robert Bamler and Stephan Mandt. Dynamic word embeddings. In *International conference on*  
492 *Machine learning*, pp. 380–389. PMLR, 2017.

493

494 Ane Blázquez-García, Angel Conde, Usue Mori, and Jose A Lozano. A review on outlier/anomaly  
495 detection in time series data. *ACM computing surveys (CSUR)*, 54(3):1–33, 2021.

496

497 D. M. Blei and J. D Lafferty. Dynamic topic models. In *Proceedings of the 23rd International*  
498 *Conference on Machine Learning*, pp. 113–120, 2006.

499

500 Tom B. Brown, Benjamin Mann, Nick Ryder, Melanie Subbiah, Jared Kaplan, Prafulla Dhariwal,  
501 Arvind Neelakantan, Pranav Shyam, Girish Sastry, Amanda Askell, et al. Language models are  
502 few-shot learners. In *Advances in Neural Information Processing Systems*, volume 33, 2020. URL  
503 <https://arxiv.org/abs/2005.14165>.

504

505 Fabio Calefato, Filippo Lanubile, and Nicole Novielli. Emotxt: A toolkit for emotion recognition  
506 from text. In *Proceedings of the Seventh International Conference on Affective Computing and*  
507 *Intelligent Interaction (ACII)*, pp. 79–85, 2017.

508

509 Yang Cao, Sikun Yang, Chen Li, Haolong Xiang, Lianyong Qi, Bo Liu, Rongsheng Li, and Ming  
510 Liu. Tad-bench: A comprehensive benchmark for embedding-based text anomaly detection. *arXiv*  
511 *preprint arXiv:2501.11960*, 2025.

512

513 Julio E Castrillón-Candás and Mark Kon. Anomaly detection: A functional analysis perspective.  
514 *Journal of Multivariate Analysis*, 189:104885, 2022.

515

516 Mariana Cavique, Antónia Correia, Ricardo Ribeiro, and Fernando Batista. What are airbnb hosts  
517 advertising? a longitudinal essay in lisbon. *Consumer Behavior in Tourism and Hospitality*, 17(3):  
518 312–325, 2022.

519

520 Wenlin Dai and Marc G Genton. Functional boxplots for multivariate curves. *Stat*, 7(1):e190, 2018.

521

522 Jacob Devlin, Ming-Wei Chang, Kenton Lee, and Kristina Toutanova. Bert: Pre-training of deep  
523 bidirectional transformers for language understanding, 2019. URL <https://arxiv.org/abs/1810.04805>.

524

525 Inderjit S Dhillon and Dharmendra S Modha. Concept decompositions for large sparse text data  
526 using clustering. *Machine learning*, 42(1):143–175, 2001.

527

528 Peter Sheridan Dodds, Kameron Decker Harris, Isabel M Kloumann, Catherine A Bliss, and Christopher M Danforth. Temporal patterns of happiness and information in a global social network:  
529 Hedonometrics and twitter. *PloS one*, 6(12):e26752, 2011.

530

531 Elizabeth Ford, John A Carroll, Helen E Smith, Donia Scott, and Jackie A Cassell. Extracting  
532 information from the text of electronic medical records to improve case detection: a systematic  
533 review. *Journal of the American Medical Informatics Association*, 23(5):1007–1015, 2016.

534

535 Daniel Gervini. Detecting and handling outlying trajectories in irregularly sampled functional datasets.  
536 *The Annals of Applied Statistics*, pp. 1758–1775, 2009.

537

538 Thomas L Griffiths and Mark Steyvers. Finding scientific topics. *PNAS*, 101(suppl. 1):5228–5235,  
539 2004.

540

541 Siteng Hao et al. Dynamic modeling for multivariate functional and longitudinal data. *Journal of*  
542 *Econometrics*, 239(2):105573, 2024. ISSN 0304-4076. doi: <https://doi.org/10.1016/j.jeconom.2023.105573>.

540 Clara Happ and Sonja Greven. Multivariate functional principal component analysis for data observed  
 541 on different (dimensional) domains. *Journal of the American Statistical Association*, 113(522):  
 542 649–659, 2018. doi: 10.1080/01621459.2016.1273115. URL <https://doi.org/10.1080/01621459.2016.1273115>.

543

544 Yupeng Hou, Jiacheng Li, Zhankui He, An Yan, Xiusi Chen, and Julian McAuley. Bridging language  
 545 and items for retrieval and recommendation. *arXiv preprint arXiv:2403.03952*, 2024.

546

547 Mia Hubert, Peter J Rousseeuw, and Pieter Segaert. Multivariate functional outlier detection. *Statisti-  
 548 cal Methods & Applications*, 24(2):177–202, 2015.

549

550 Clayton J Hutto, Sarita Yardi, and Eric Gilbert. A longitudinal study of follow predictors on twitter.  
 551 In *Proceedings of the sigchi conference on human factors in computing systems*, pp. 821–830,  
 552 2013.

553

554 Ramakrishnan Kannan, Hyenkyun Woo, Charu C Aggarwal, and Haesun Park. Outlier detection for  
 555 text data. In *Proceedings of the 2017 siam international conference on data mining*, pp. 489–497.  
 556 SIAM, 2017.

557

558 Sean W Kelley and Claire M Gillan. Using language in social media posts to study the network  
 559 dynamics of depression longitudinally. *Nature communications*, 13(1):870, 2022.

560

561 Minhee Kim et al. Covariate dependent sparse functional data analysis. *INFORMS Journal on Data  
 562 Science (IJDS) (Online)*, 2, 2023.

563

564 Nan M Laird and James H Ware. Random-effects models for longitudinal data. *Biometrics*, pp.  
 565 963–974, 1982.

566

567 Yinhai Liu, Myle Ott, Naman Goyal, Jingfei Du, Mandar Joshi, Danqi Chen, Omer Levy, Mike  
 568 Lewis, Luke Zettlemoyer, and Veselin Stoyanov. Roberta: A robustly optimized bert pretraining  
 569 approach, 2019. URL <https://arxiv.org/abs/1907.11692>.

570

571 Yu-Bao Liu, Jia-Rong Cai, Jian Yin, and Ada Wai-Chee Fu. Clustering text data streams. *Journal of  
 572 computer science and technology*, 23(1):112–128, 2008.

573

574 Yu Lu and Harrison H Zhou. Statistical and computational guarantees of lloyd’s algorithm and its  
 575 variants. *arXiv preprint arXiv:1612.02099*, 2016.

576

577 Saif M. Mohammad. Practical and ethical considerations in the effective use of emotion and sentiment  
 578 lexicons. In *Proceedings of the 12th Language Resources and Evaluation Conference*, pp. 4543–  
 579 4549, 2020.

580

581 Saif M. Mohammad and Felipe Bravo-Marquez. Emotion intensities in tweets. *Proceedings of  
 582 NAACL-HLT*, pp. 1–6, 2018.

583

584 Hans-Georg Müller. Functional modelling and classification of longitudinal data. *Scandinavian  
 585 Journal of Statistics*, 32(2):223–240, 2005.

586

587 Brendan O’Connor, Ramnath Balasubramanyan, Bryan Routledge, and Noah Smith. From tweets to  
 588 polls: Linking text sentiment to public opinion time series. In *Proceedings of the international  
 589 AAAI conference on web and social media*, volume 4, pp. 122–129, 2010.

590

591 Robert Plutchik. Emotion: Theory, research, and experience. *Theories of emotion*, 1, 1980.

592

593 Lukas Ruff, Yury Zemlyanskiy, Robert Vandermeulen, Thomas Schnake, and Marius Kloft. Self-  
 594 attentive, multi-context one-class classification for unsupervised anomaly detection on text. In  
 595 *Proceedings of the 57th Annual Meeting of the Association for Computational Linguistics*, pp.  
 596 4061–4071, 2019.

597

598 Amandine Schmutz, Julien Jacques, Charles Bouveyron, Laurence Cheze, and Pauline Martin.  
 599 Clustering multivariate functional data in group-specific functional subspaces. *Computational  
 600 Statistics*, 35(3):1101–1131, 2020.

601

602 Six Seconds. Plutchik’s wheel of emotions: Feelings wheel, 2025. URL <https://www.6seconds.org/2025/02/06/plutchik-wheel-emotions/>. Accessed 2025-05-21.

594 Alfonso Semeraro, Salvatore Vilella, and Giancarlo Ruffo. Pyplutchik: Visualising and comparing  
 595 emotion-annotated corpora. *PLOS ONE*, 16(9):e0256503, September 2021. ISSN 1932-6203. doi:  
 596 10.1371/journal.pone.0256503. URL <http://dx.doi.org/10.1371/journal.pone.0256503>.

598 Alvin Subakti, Hendri Murfi, and Nora Hariadi. The performance of bert as data representation of  
 599 text clustering. *Journal of big Data*, 9(1):15, 2022.

601 Ying Sun and Marc G Genton. Functional boxplots. *Journal of computational and graphical statistics*,  
 602 20(2):316–334, 2011.

603 Danny Valdez, Marijn Ten Thij, Krishna Bathina, Lauren A Rutter, and Johan Bollen. Social media  
 604 insights into us mental health during the covid-19 pandemic: longitudinal analysis of twitter data.  
 605 *Journal of medical Internet research*, 22(12):e21418, 2020.

607 Geert Verbeke, Steffen Fieuws, Geert Molenberghs, and Marie Davidian. The analysis of multivariate  
 608 longitudinal data: a review. *Statistical methods in medical research*, 23(1):42–59, 2014.

609 Xuerui Wang and Andrew McCallum. Topics over time: a non-markov continuous-time model of  
 610 topical trends. KDD '06, pp. 424–433, New York, NY, USA, 2006. Association for Computing  
 611 Machinery. ISBN 1595933395. URL <https://doi.org/10.1145/1150402.1150450>.

613 Shushan Wu, Luyang Fang, Jinan Zhang, TN Sriram, Stephen J Coshatt, Feraidoon Zahiri, Alan Man-  
 614 tooth, Jin Ye, Wenxuan Zhong, Ping Ma, et al. Unsupervised anomaly detection and diagnosis in  
 615 power electronic networks: Informative leverage and multivariate functional clustering approaches.  
 616 *IEEE Transactions on Smart Grid*, 15(2):2214–2225, 2023.

617 Jiehui Xu, Haixu Wu, Jianmin Wang, and Mingsheng Long. Anomaly transformer: Time series  
 618 anomaly detection with association discrepancy, 2022. URL <https://arxiv.org/abs/2110.02642>.

621 Kenneth CC Yang and Yowei Kang. What can college teachers learn from students' experiential nar-  
 622 ratives in hybrid courses?: A text mining method of longitudinal data. In *Theoretical and practical  
 623 approaches to innovation in higher education*, pp. 91–112. IGI Global Scientific Publishing, 2020.

624 Fang Yao, Hans-Georg Müller, and Jane-Ling Wang. Functional data analysis for sparse longitudinal  
 625 data. *Journal of the American Statistical Association*, 100(470):577–590, 2005. doi: 10.1198/  
 626 016214504000001745. URL <https://doi.org/10.1198/016214504000001745>.

627 Jianhua Yin and Jianyong Wang. A model-based approach for text clustering with outlier detection.  
 628 In *2016 IEEE 32nd International Conference on Data Engineering (ICDE)*, pp. 625–636. IEEE,  
 629 2016.

631 Mikhail Yurochkin, Zhiwei Fan, Aritra Guha, Paraschos Koutris, and XuanLong Nguyen. Scalable  
 632 inference of topic evolution via models for latent geometric structures. In *Advances in Neural  
 633 Information Processing Systems*, 32, 2019.

634 Zahra Zamanzadeh Darban, Geoffrey I Webb, Shirui Pan, Charu Aggarwal, and Mahsa Salehi. Deep  
 635 learning for time series anomaly detection: A survey. *ACM Computing Surveys*, 57(1):1–42, 2024.

637 Yidong Zhou and Hans-Georg Mueller. Dynamic modelling of sparse longitudinal data and functional  
 638 snippets with stochastic differential equations. *Journal of the Royal Statistical Society Series B:  
 639 Statistical Methodology*, pp. qkae116, 2024.

640  
 641  
 642  
 643  
 644  
 645  
 646  
 647